Real-time monitoring of cell viability by its nanoscale height change with oxygen as endogenous indicator†

Yadong Xue,[a] Jianping Lei,[a] Xu Xu,[a] Lin Ding,[a] Chun Zhai,[a] Feng Yan[b] and Huangxian Ju*[a]

Received 2nd June 2010, Accepted 19th August 2010
DOI: 10.1039/c0cc01700k

A method for real-time evaluation of cell viability was developed by using oxygen as an endogenous indicator in scanning electrochemical microscopy to monitor the nanoscale height change of a single cell in a physiological environment with a novel Pt nanodisk electrode and a newly designed step-approaching strategy.

Scanning electrochemical microscopy (SECM) has been extensively applied in biological analysis such as measuring catalytic activity,[1] monitoring the metabolism,[2] investigating the neurotransmitter secretion,[3] and imaging the morphology[4] due to its ability in quantitative measurements of both intercellular and intracellular physiological processes.[5] Unlike scanning ion conductance microscopy,[6] these measurements usually need an exogenous redox indicator, such as $Fe(CN)_6^{4-}$ or $Ru(NH_3)_6^{3+}$ for morphological imaging,[2b,3a,4] which makes it difficult to essentially exhibit the long-time state of cells due to the poor biocompatibility and toxicity of these indicators. Although atomic force microscopy (AFM) has been applied for high-resolution imaging of living cells,[7] the physical interaction of AFM may cause unexpected changes in cells.[4d] Thus, so far little attention has been paid to the long-time cell height change concerned with viability in a physiological environment. To address this issue, it is imperative to search for a biocompatible indicator for SECM analysis.

Oxygen has been used as a redox probe for SECM study of the local catalytic activity of some biocatalytic systems.[1c] The formation[2b] and consumption[2c] of oxygen in cellular physiological processes have also been investigated by SECM. Since the oxygen reduction signal in SECM constant-height mode is usually composed of morphological effect and biological origin,[4b] this work designed a step-approaching strategy to distinguish the multiplex signals, and then used oxygen as an endogenous indicator for noninvasive SECM detection of cell height change.

In order to obtain high spatial and temporal resolution for single-cell SECM analysis,[4b,c] this work firstly proposed a simple method for preparation of Pt nanodisk tips using a laser puller.[8] The tips were prepared by assembling a Pt wire-inserted quartz capillary in a borosilicate glass tube for improving the ductibility (Fig. S1 in ESI†). Scanning electron microscopic images of the resulting Pt nanodisk tip showed an abrupt decrease of the tip diameter in the heating zone and an exposed Pt nanodisk (Fig. S2 in ESI†). The effective radius could be down to 5 nm calculated from the steady-state response of a redox probe. Considering that a small electrode had limited imaging range in constant-height mode,[4b] a 400-nm-radius tip was used in the work, and a potential of −0.4 V was applied for oxygen reduction (Fig. S3 in ESI†).

Adherent BGC-823 human gastric carcinoma (BGC) cells were chosen as a model target for morphological study in phosphate-buffered saline (PBS). When the tip was laterally scanned in a horizontal (x–y) plane above a single BGC cell, the reduction current of oxygen was recorded as i_T, which gave a negative peak i_P at the center of the cell (Fig. 1a). A typical SECM image of a single BGC cell in PBS is shown in Fig. 1c. Although slight instability of the tip current was observed on the edge as reported by Bard's group,[9a] currents around the cell were steady. The cell center taken by SECM was much darker than the edge, indicating the decrease of current, which apparently originated from three parts: (1) negative feedback effect due to cell morphology, (2) consumption due to cell respiration, (3) permeability for oxygen due to natural diffusion and SECM-induced transfer.[9b] Parts (2) and (3) could be involved in the net flux of oxygen through the cell membrane.

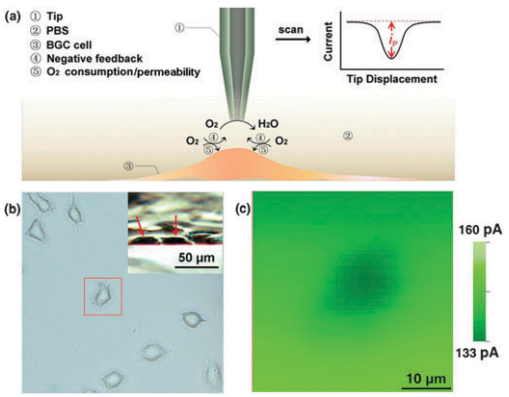

Fig. 1 (a) Schematic representation of the feedback mode SECM experiment with single BGC cell *via* oxygen as endogenous indicator. (b) Optical microscopic and (c) SECM images of single BGC cell. SECM conditions: tip radius, 400 nm; tip potential, −0.4 V *vs.* Ag/AgCl; scan rate, 25 μm s^{-1}; rest time, 2 min. Inset in (b) shows lateral micrograph of BGC cells (red arrow) spreading on petri dish.

[a] *Key Laboratory of Analytical Chemistry for Life Science (Ministry of Education of China), Department of Chemistry, Nanjing University, Nanjing 210093, P. R. China. E-mail: hxju@nju.edu.cn; Fax: +86 25 83593593; Tel: +86 25 83593593*
[b] *Jiangsu Institute of Cancer Prevention and Cure, Nanjing 210009, P. R. China*

† Electronic supplementary information (ESI) available: Experimental details, fabrication and characterization of Pt nanodisk electrodes, optical characterization of cell apoptosis, examination of tip drift and effect of paclitaxel. See DOI: 10.1039/c0cc01700k

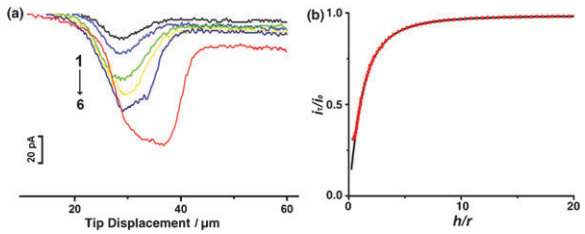

Fig. 2 (a) Typical SECM single-line scan curves over single cell at different tip–cell distances decreasing from curves 1 to 6. The steady-state current in bulk solution was 169 pA. (b) Plot of normalized current (i_T/i_0) *vs.* normalized distance (h/r) at a 400-nm-radius Pt-disk tip approaching to the petri dish bottom in PBS. i_0, steady-state reduction current measured in bulk solution; h, tip–substrate distance; r, tip radius. Solid line is the theory curve (RG $\geq$ 10), and dots are the experiment data.

A step-approaching method was thus proposed to distinguish the component i_d caused by the negative feedback effect of cell morphology and the contribution of oxygen flux through the cell membrane, i_f. Assuming that the SECM image was obtained at a height h from the petri dish bottom, the corresponding one-line scan curve with a negative peak i_P was recorded (curve 1 in Fig. 2a). The tip was then scanned at decreasing heights to obtain a series of negative peaks. With the decreasing tip height, the negative peak increased. When the tip reached a comparative height to the cell, a slight tip–cell contact occurred, which led to a drift of the peak position (curve 6 in Fig. 2a). The total height decrease d of the tip from h (curve 1) to tip–cell contact (curve 6) was just the approximation of tip–cell distance in the SECM image. To avoid the error resulting from the contact, the step-approaching was accurately monitored by the single-line scan curve.

On the other hand, the amperometric approach curve to the petri dish bottom in PBS was recorded to characterize the dependence of the negative feedback effect on tip–substrate distance. The theory approach curve to an insulating substrate for the disk-shaped tip with RG $\geq$ 10 (RG, the ratio of the overall radius to the radius of the conductor) should accord with the following equation[10]

$$i_T(L)/i_0 = 1/\{0.15 + 1.5385/L + 0.58\exp(-1.14/L) + 0.0908\exp[(L - 6.3)/(1.017L)]\}$$

where L is the normalized distance between the insulating substrate and the tip of radius r, and i_0 is the steady-state current. A perfect fit between the experimental data and the theoretical curve is shown in Fig. 2b, suggesting the reliability of the quantitative analysis.

As shown in the inset in Fig. 1b, the top surface of adherent BGC cells was flat. Assuming the cell was an insulator, the negative feedback effect to both petri dish and center of a cell should be essentially identical.[1a] This could be verified by approaching the tip to the BGC cell surface using $Fe(CN)_6^{3-}$ as the indicator (Fig. S4 in ESI†). Based on this conclusion, i_d caused by the negative feedback effect of the cell could be obtained from the approach curve to the petri dish bottom (Fig. 2b) and d value. Thus, i_f corresponding to the oxygen flux of the living cell could be calculated using $i_f = i_P - i_d$. The results showed that the ratio of i_d to i_f was in the range of 10 : 1 to 5 : 1 (Table 1), indicating that cell morphology was the key factor responsible for current decrease i_P in this work. In addition, the vertical distance from tip to cell surface was within 2 μm during all the SECM measurements in this work. In order to visualize the change in cell height, SECM images after subtracting the baseline current were shown in a subsequent time-course study.

Table 1 Evaluation of i_d and i_f corresponding to negative feedback effect and oxygen flux through cell membrane using 6 BGC cells

Cell	i_0/pA	i_T/pA	d/μm	i_d/pA	i_f/pA
1	168	120	0.86	42.4	5.6
2	170	135	1.05	30.3	4.8
3	167	107	0.68	53.2	5.0
4	169	110	0.74	52.7	6.3
5	170	134	1.20	29.1	5.4
6	171	131	1.10	33.7	6.1

Consecutive optical observation did not show the apparent morphological change of BGC cells exposed to 25 °C PBS in 2 h (Fig. S5 in ESI†). However, a time course of the decrease in oxygen reduction current around a single BGC cell at different time intervals could be sensitively obtained by the repetitive scan of the SECM tip (Fig. 3). During the exposure to 25 °C PBS for 2 h (images a to q in Fig. 3), a continuous increase of i_P as well as cell size was distinctly observed till a tip–cell contact occurred (images q–t in Fig. 3).

To identify the stability of z-piezo for the SECM experiment, a micrometre-sized polydimethylsiloxane (PDMS) protrusion on a petri dish was chosen as model insulator to study the drift of the SECM tip, since the oxygen solubility and permeability of the PDMS were not expected to change with time. No obvious change of peak current was observed when the tip was scanned above the PDMS protrusion in 2 h (Fig. S6 in ESI†), identifying neglectable z-piezo drift during the whole scan. Therefore, cell height increased gradually with the exposure time, indicating the morphological change of the adherent cell. This change resulted from the early apoptosis of BGC cells in PBS, which was characterized with an Annexin V-FITC apoptosis detection kit coupled with a confocal fluorescent microscope (Fig. S7 in ESI†).[11] Although the signals were weak, the confocal fluorescent images showed an early apoptosis of BGC cells within 3 h, in which the propidine iodide staining experiment showed the cell

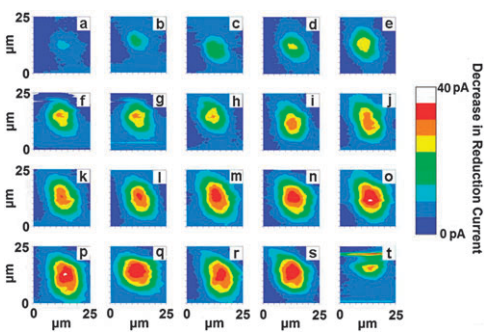

Fig. 3 Sequential SECM images of BGC cell obtained with a 400-nm-radius Pt tip at every 7.5 min from (a) 0 to (t) 142.5 min in PBS solution. The tip was scanned at 25 μm s^{-1} with a fixed potential of −0.4 V *vs.* Ag/AgCl and the rest time was 2 min. The steady-state current in bulk solution was 169 pA.

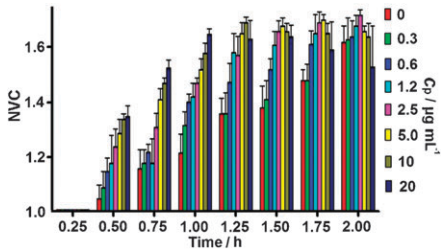

Fig. 4 Plots of NVC *vs.* treatment time at different paclitaxel concentrations from 0 to 20 μg mL^{-1} at ambient temperature. SECM measurements were recorded with a 400-nm-radius Pt tip at −0.4 V *vs.* Ag/AgCl with a scan rate of 25 μm s^{-1}.

membrane was intact. However, the early apoptosis could weaken its adhesion ability,[12] producing the increase of cell height, which should be responsible to the variation of i_d.

From the similar i_f values obtained for different cells (Table 1), oxygen distribution caused by cell consumption could be the same when the tip was close to the cell surface (< 2 μm).[2c] Furthermore, considering the fact that the cell membrane remained intact (Fig. S7 in ESI†), the respiratory ability of cells in early apoptosis was almost constant.[13] Since the proportion of i_f to i_d was relatively small (<20%), i_f at different time intervals could be regarded as invariable throughout the time-course study. Using the step-approaching method at the end of each time course to separate i_d from the detectable i_P by deducting the contribution of oxygen flux i_f, a series of i_d values at different time intervals were obtained. It should be mentioned that the step-approaching procedure was operated at the end of each time course to prevent a possible biological effect caused by mechanically touching the cell. Thus the height change of BGC cells exposed to 25 °C PBS in 2 h was estimated to be in the range of 55 to 365 nm (n = 8), which was smaller than the height change of 0.75 to 1 μm when living PC12 cells were exposed to hypotonic and hypertonic solutions.[4a] This is the first long-time investigation of nanoscale cell height change in a physiological environment.

To validate the origin of cell height change, paclitaxel was chosen to treat BGC cells for monitoring cell viability, which is related to the total biological activities of cells. Time courses of paclitaxel treatment at different concentrations showed the height change was accelerated with the increasing paclitaxel concentration (c_p) (Fig. S8 in ESI†), which could be attributed to the function of paclitaxel as apoptosis-inducer.[14]

For evaluating the effect of paclitaxel on cell height change, a normalized variation of peak current (NVC) was defined as: $(i_{P,t} - i_{P,0})/(i_{P,1} - i_{P,0})$ (Fig. 4). Here, $i_{P,t}$, $i_{P,1}$ and $i_{P,0}$ are the peak currents at time intervals t, 15 and 0 min, respectively. The NVCs of BGC cells exposed to paclitaxel at c_p > 2.5 μg mL^{-1} quickly increased to reach a plateau value of 1.7. In the absence of paclitaxel, the NVC also increased to the plateau value with a longer time. This resulted from the early apoptosis of cells in PBS (Fig. S7 in ESI†). The drug sensitivity test by MTT assay demonstrated the increasing cytotoxicity with the increasing c_p from 0 to 2.5 μg mL^{-1} (Fig. S9 in ESI†). Thus, SECM measurements could sensitively monitor the cell viability of adherent cells exposed to different environments by real-time monitoring of their nanoscale height changes, and evaluate the drug sensitivity of paclitaxel on inducing apoptosis.

In summary, the nanoscale height change of a single cell related to cell viability can be sensitively monitored by SECM with oxygen as an endogenous indicator. A simple approach is proposed for the fabrication of a Pt nanodisk electrode, which shows good reproducibility and controllable radius down to 5 nm. The multiple oxygen reduction current during SECM constant-height scan can be separated with the proposed step-approaching method. The oxygen indicator avoids the interference of other exogenous species. The practicability of the designed strategy has been demonstrated by treating model cells with paclitaxel and real-time SECM monitoring. This work would attract attention to the long-time morphological change of cells concomitant with their viability.

This work was supported by National Natural Science Foundation of China (20821063, 90713015, 20875044) and National Basic Research Program of China (2010CB732400).

Notes and references

1 (*a*) B. Liu, S. A. Rotenberg and M. V. Mirkin, *Proc. Natl. Acad. Sci. U. S. A.*, 2000, **97**, 9855–9860; (*b*) G. Wittstock, M. Burchardt, S. E. Pust, Y. Shen and C. Zhao, *Angew. Chem., Int. Ed.*, 2007, **46**, 1584–1617; (*c*) K. Karnicka, K. Eckhard, D. A. Guschin, L. Stoica, P. J. Kulesza and W. Schuhmann, *Electrochem. Commun.*, 2007, **9**, 1998–2002.

2 (*a*) J. Mauzeroll, A. J. Bard, O. Owhadian and T. J. Monks, *Proc. Natl. Acad. Sci. U. S. A.*, 2004, **101**, 17582–17587; (*b*) T. Yasukawa, T. Kaya and T. Matsue, *Anal. Chem.*, 1999, **71**, 4637–4641; (*c*) H. Shiku, T. Shiraishi, H. Ohya, T. Matsue, H. Abe, H. Hoshi and M. Kobayashi, *Anal. Chem.*, 2001, **73**, 3751–3758.

3 (*a*) A. Hengstenberg, A. Blöchl, I. D. Dietzel and W. Schuhmann, *Angew. Chem., Int. Ed.*, 2001, **40**, 905–908; (*b*) S. Isik and W. Schuhmann, *Angew. Chem., Int. Ed.*, 2006, **45**, 7451–7454.

4 (*a*) J. M. Liebetrau, H. M. Miller, J. E. Baur, S. A. Takacs, V. Anupunpisit, P. A. Garris and D. O. Wipf, *Anal. Chem.*, 2003, **75**, 563–571; (*b*) R. T. Kurulugama, D. O. Wipf, S. A. Takacs, S. Pongmayteegul, P. A. Garris and J. E. Baur, *Anal. Chem.*, 2005, **77**, 1111–1117; (*c*) P. Sun, F. O. Laforge, T. P. Abeyweera, S. A. Rotenberg, J. Carpino and M. V. Mirkin, *Proc. Natl. Acad. Sci. U. S. A.*, 2008, **105**, 443–448; (*d*) A. Ueda, O. Niwa, K. Maruyama, Y. Shindo, K. Oka and K. Suzuki, *Angew. Chem., Int. Ed.*, 2007, **46**, 8238–8241.

5 R. M. Wightman, *Science*, 2006, **311**, 1570–1574.

6 A. I. Shevchuk, G. I. Frolenkov, D. Sánchez, P. S. James, N. Freedman, M. J. Lab, R. Jones, D. Klenerman and Y. E. Korchev, *Angew. Chem., Int. Ed.*, 2006, **45**, 2212–2216.

7 A. Sharma, K. I. Anderson and D. J. Muller, *FEBS Lett.*, 2005, **579**, 2001–2008.

8 (*a*) Y. H. Shao, M. V. Mirkin, G. Fish, S. Kokotov, D. Palanker and A. Lewis, *Anal. Chem.*, 1997, **69**, 1627–1634; (*b*) B. B. Katemann and W. Schuhmann, *Electroanalysis*, 2002, **14**, 22–28; (*c*) Y. Li, D. Bergman and B. Zhang, *Anal. Chem.*, 2009, **81**, 5495–5502.

9 (*a*) A. J. Bard, X. Li and W. Zhan, *Biosens. Bioelectron.*, 2006, **22**, 461–472; (*b*) A. L. Barker, J. V. Macpherson, C. J. Slevin and P. R. Unwin, *J. Phys. Chem. B*, 1998, **102**, 1586–1598.

10 M. V. Mirkin, F.-R. F. Fan and A. J. Bard, *J. Electroanal. Chem.*, 1992, **328**, 47–62.

11 T. Rudel and G. M. Bokoch, *Science*, 1997, **276**, 1571–1574.

12 H. P. Dong, L. Kleinberg, B. Davidson and B. Rrisberg, *Nat. Protoc.*, 2008, **3**, 955–964.

13 (*a*) L. Troiano, R. Ferraresi, E. Lugli, E. Nemes, E. Roat, M. Nasi, M. Pinti and A. Cossarizza, *Nat. Protoc.*, 2007, **2**, 2719–2727; (*b*) A. Cossarizza, G. Kalashnikova, E. Grassilli, F. Chiappelli, S. Salvioli, M. Capri, D. Barbieri, L. Troiano, D. Monti and C. Franceschi, *Exp. Cell Res.*, 1994, **214**, 323–330; (*c*) N. Zamzami, P. Marchetti, M. Castedo, C. Zanin, J.-L. Vayssière, P. X. Petit and G. Kroemer, *J. Exp. Med.*, 1995, **181**, 1661–1672.

14 M. Motwani, T. M. Delohery and G. K. Schwartz, *Clin. Cancer Res.*, 1999, **5**, 1876–1883.

Electronic Supplementary Information (ESI) for Chemical Communications

Real-Time Monitoring of Cell Viability by Its Nanoscale Height Change with Oxygen as Endogenous Indicator

Yadong Xue, Jianping Lei, Xu Xu, Lin Ding, Chun Zhai, Feng Yan and Huangxian Ju*

Key Laboratory of Analytical Chemistry for Life Science (Education Ministry of China), Department of Chemistry, Nanjing University, Nanjing 210093, P.R. China; and Jiangsu Institute of Cancer Prevention and Cure, Nanjing 210009, P.R. China

Experimental details

Chemicals and materials. 3-(4,5-Dimethylthiazol-2-yl)-2,5-diphenyltetrazolium bromide (MTT) and Annexin V-FITC apoptosis detection kit were purchased from Sigma (St. Louis, MO, USA). Paclitaxel was acquired from Taiji Pharmaceutical Limited (Sichuan, China). 0.01 M pH 7.4 phosphate-buffered saline (PBS) containing 136.7 mM NaCl, 2.7 mM KCl, 87 mM Na_2HPO_4, and 14 mM KH_2PO_4 was sterilized before use. All aqueous solutions were prepared using ≥18 MΩ ultrapure water purified with a Millipore Milli-Q system. All other reagents were of at least reagent grade quality.

Pt wire with a diameter of 50 μm (purity 99.9%, hard) was provided by Alfa Aesar (Ward Hill, MA, USA). Borosilicate glasses with a length of 100 mm, an outer diameter of 1 mm and an inner diameter of 500 μm were purchased from Sutter Instrument Company (Novata, CA, USA). The quartz capillaries were obtained from Yongnian Optic Fiber Plant (Hebei, China) with an outer diameter of 375 μm and an inner diameter of 100 μm.

Apparatus. A Sutter P-2000 laser puller was used for the fabrication of nanoelectrodes. The subsequent polishing procedure was accomplished by a microforge MF-900 (Marishige, Tokyo, Japan). The Pt tip

image was obtained with S-4800 scanning electron microscope (SEM) (Hitachi, Japan). Brightfield and fluorescence images were taken by virtue of TE2000-U inverted fluorescence microscope (Nikon, Japan) and Leica TCS SP5 laser scanning confocal microscope (Germany). Cyclic voltammetry (CV) was performed with a three-electrode system by using a CHI 660 electrochemical analyzer (USA) equipped with a Faraday cage. A two-electrode setup comprising a 0.25-mm Ag/AgCl reference electrode and a Pt nanodisk electrode as working electrode was employed for scanning electrochemical microscopic (SECM) measurements on CHI 900 scanning electrochemical microscope (Austin, TX, USA), which was mounted on the horizontal stage of an inverted biological microscope set on a rigid aluminum platform. According to user's manual for CHI900B SECM, the *z*-piezo can travel 85 μm with a resolution down to a nanometer.

Fabrication of Pt nanodisk electrodes. Fig. S1 represents the fabrication procedure of Pt nanodisk electrodes. A 25-mm-length platinum wire was cut and inserted into a 15-mm-length quartz capillary with the polyimide layer burned off, so that about 5 mm of platinum wire protruded from both ends. Then, the capillary was inserted into a 100-mm-length borosilicate glass tube. The resulting glass/quartz/wire assembly was placed inside the laser heating chamber so that the laser beam was focused on the center of the quartz capillary. To avoid any pulling force on the glass capillary, two plastic tubes were used to hold the sleighs of the puller tightly.

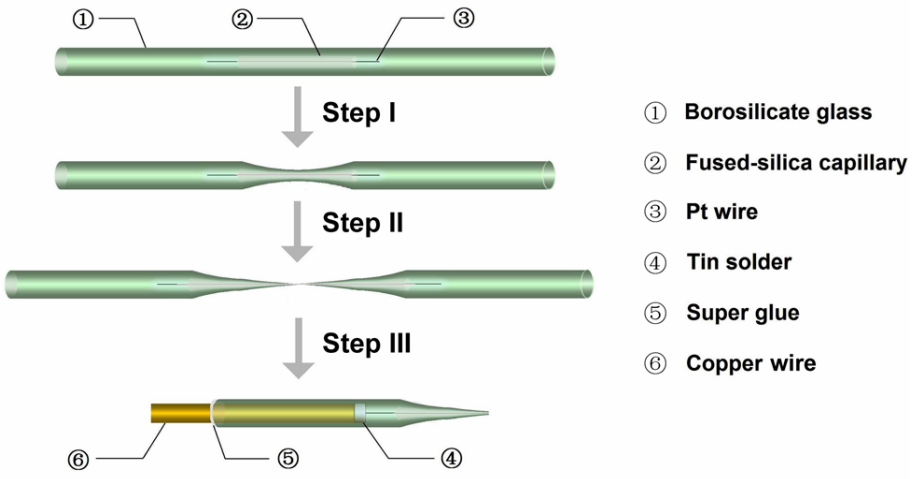

Fig. S1 Schematic diagram of the fabrication procedure of nanoelectrode tip. Steps I, II and III represent the process of fusing, pulling, and polishing and connecting, respectively.

In Step I, a program which consisted of only one line with the following parameter set was loaded, "heat: 750, filament: 5, velocity: 10, delay: 128, pull: 0". After heating for 10 s, the program of the laser puller was interrupted for a period of 20 s to allow the assembly to cool down and prevent overheating of the laser. This procedure was thrice repeated in order to assure an optimal sealing of the Pt wire inside the quartz capillary. After borasilicate glass was rotated by 180°, thrice repeated heating was carried out again for uniform heating. In Step II, two plastic tubes were firstly removed, and the second program "heat: 800, filament: 1, velocity: 130, delay: 124, pull: 220" was started to obtain two Pt nanowires sealed tightly in the capillary. Afterwards, Step III was performed for polishing and electrical connection. Polishing step was performed in a drop of water by slowly lowering down the tip-holder onto a polishing plate using manual micropositioning elements. Electrical contact to the Pt wire was established with a copper wire and a piece of tin solder. Finally, super glue was used to seal the opening end. Prior to use, a pretreatment was needed for the activation of Pt nanodisk electrode, by cyclic voltammetric sweeping between −0.2 and +1.2 V in 0.5 M H_2SO_4 solution for 30 min. After each SECM experiment, the electrode was immersed in 30% nitric acid for 30 min to eliminate the possible contamination of the electrode.

Cell culture and preparation. The BGC cell line was kindly provided by Affiliated Zhongda Hospital of Southeast University, Nanjing, China. BGC cells were cultured in a flask in RPMI 1640 medium (GIBCO) supplemented with 10% fetal calf serum (FCS, Sigma), penicillin (100 μg mL^{-1}), and streptomycin (100 μg mL^{-1}) at 37 °C in a humidified atmosphere containing 5% CO_2. 1.0×10^5 cells were then transferred into a polystyrene petri dish (Corning Incorporated, NY, USA) to culture for another 24 h, after which the BGC cells could attach to the bottom with a surface density of 5.0×10^3 cells cm^{-2} approximately.

SECM procedure. Prior to each SECM experiment, the adherent cells were twice washed with 37 °C PBS. The petri dish was filled with 4 mL PBS and mounted on the horizontal stage of SECM. The precipitation of calcium leaking from the cells was neglectable due to the very low amount of calcium

relative to the volume of testing solution. Firstly, the tip current (i_T) for reduction of dissolved oxygen at –0.4 V was recorded as a function of the tip position when the tip was scanned down to the petri dish vertically by a motor-driven XYZ stage. After stopped at 60% of the steady-state current, the sensing tip was retracted to a 14-μm separation from the petri dish (the average height of cells was 12 μm). Then, with the help of optical microscopy, single-line scan was operated laterally above the cell surface to get the profile of i_T versus the displacement of the tip along *x* axis. The optimal tip height (*h*) was obtained by gradually approaching the tip along *z* axis to the cell (every 100 nm), until a peak appeared on the single-line scan curve with the signal-to-noise ratio larger than 10. The SECM images were then recorded by continuously scanning over the BGC cells at a scan rate of 25 μm s^{-1} in the constant-height mode. The scan range was 60 μm × 60 μm. The time required to obtain one whole SECM image was about 5 min.

Fluorescent measurements of cell apoptosis. Annexin V-FITC apoptosis detection kit is used to observe early apoptosis of cells. A series of adherent BGC cells were firstly exposed to 25 °C PBS for 0, 1, 2, 3, 4, 5 and 6 h, respectively, and then the BGE cells were stained by Annexin V-FITC apoptosis detection kit on the bottom of the petri dish. After reaction for 5 min in the dark, BGC cells covered with a slide were imaged by laser scanning confocal microscopy.

MTT assay. BGC cells (1.0×10^5) in 200 μL of either medium alone or medium containing drugs at various concentrations were added to each well of a 96-well plate. The plate was incubated at 37 °C in a humidified atmosphere of 5% CO_2 for three days. MTT (20 μL, 5 mg mL^{-1}) was then added to each well. After the plate was incubated for a further 4 h, sodium dodecyl sulfate (150 μL, 0.52 M) was added to each well to solubilize the formazan dye. After 1 h the absorbance of the control and drug-treated wells was measured by using Hitachi/Roche System Cobas 6000 (Tokyo, Japan) at 490 nm. The cytotoxicity of the drug was calculated as follows:[1]

$$\text{Cytotoxicity (\%)} = 1 - \frac{\text{absorbance of drug-treated well}}{\text{absorbance of control well}} \times 100$$

Characterization of Pt nanodisk electrodes

Pt nanodisk electrodes were characterized by SEM and CV. Fig. S2a shows an abrupt decrease of the tip diameter in the heating zone. The stretched-out tip with the shape of symmetrical taper allowed its wide application in SECM measurements. SEM at higher magnification clearly identified a Pt nanodisk with 400 nm radius in the insulating glass sheath (Fig. S2b).

The ideal sigmoidal voltammograms of as-prepared Pt nanodisk electrodes in 0.1 M KCl containing 1 mM $K_3Fe(CN)_6$ were shown in Fig. S2c. The disk sizes could be obtained from the steady-state currents and following equation[2]

$$i_{T,\infty}=4nFDcr$$

where n is electron number transferred per molecule, F is the Faraday's constant, D and c are the diffusion coefficient and bulk concentration of the electroactive species, respectively, and r is the electrode radius. The effective radius of the prepared Pt nanodisk electrodes could be down to 5 nm.

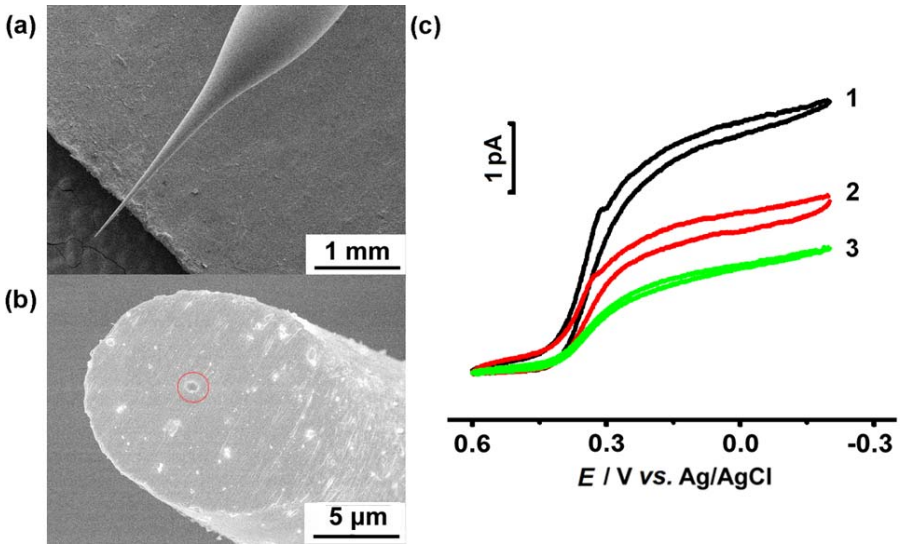

Fig. S2 SEM images of (a) taper-shaped nanoelectrode tip and (b) the front end of a tip, and (c) cyclic voltammograms of 1 mM $K_3Fe(CN)_6$ in 0.1 M KCl as supporting electrolyte at Pt nanodisk electrodes with different radii of (1) 32 nm, (2) 12 nm, (3) 5 nm. Scan rate, 50 mV s^{-1}.

Response of Pt nanodisk electrode to oxygen reduction

The Pt nanodisk electrode showed sensitive response to oxygen reduction with a maximum reduction current at -0.4 V vs. Ag/AgCl.

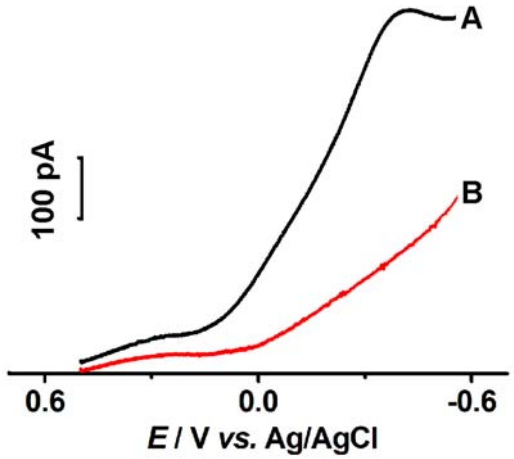

Fig. S3 Cathodic sweep curves of Pt nanodisk electrode with a radius of 400 nm in (A) air-saturated PBS and (B) PBS deaerated with nitrogen for 5 min at 30 mV s^{-1}.

Approach curve to the center of BGC cell surface using $Fe(CN)_6^{3-}$ as the indicator

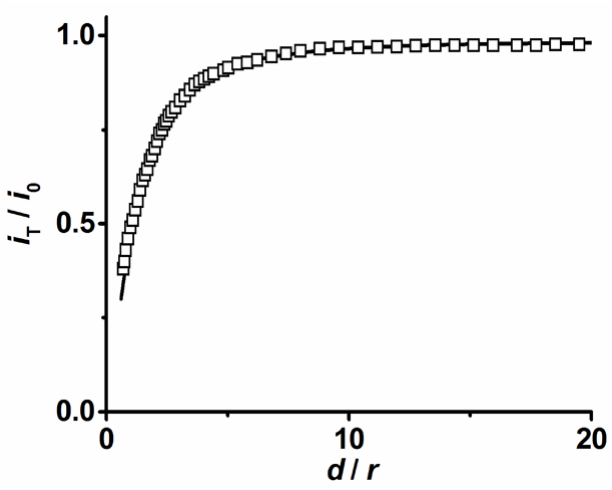

Fig. S4 Plot of normalized current (i_T/i_0) *vs.* normalized distance (d/r) at a 400-nm-radius Pt-disk tip approaching to the center of BGC cell in PBS containing 0.1 mM $K_3Fe(CN)_6$. Potential, 0.1 V *vs.* Ag/AgCl; i_0, steady-state reduction current measured in bulk solution; d, tip-cell distance; r, tip radius. The result shows that the experimental approach curve to BGC cell (grids) fits the theory curve to a planar surface for RG $\geqslant$ 10 (solid line).

Single BGC cell imaged by brightfield microscope

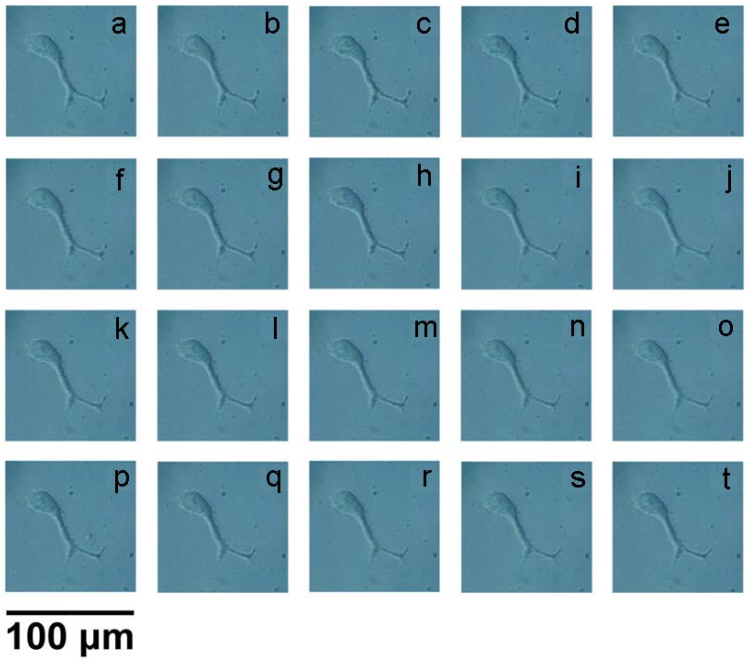

Fig. S5 Sequential brightfield images of single BGC cell taken by inverted fluorescence microscope in 25 °C PBS at every 7.5 min from (a) 0 to (t) 142.5 min.

Examination of tip drift

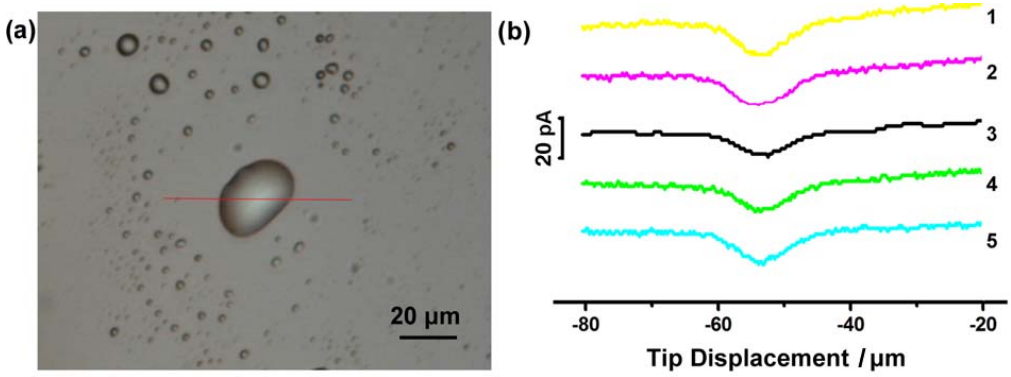

Fig. S6 (a) Optical image of the PDMS protrusion on a petri dish. (b) Consecutive constant-height SECM scan curves along the red line at (1) 0, (2) 0.5, (3) 1, (4) 1.5, and (5) 2 h. SECM measurements were performed in PBS solution with a 400-nm-radius Pt tip at −0.4 V *vs.* Ag/AgCl with a scan rate of 25 µm s^{-1}. The steady-state current in bulk solution was 171 pA.

Fluorescent images characterizing early apoptosis of BGC cells

Once the membrane phospholipids phosphatidylserine translocates from the inner face of the plasma membrane to the cell surface during early apoptosis, it can be detected by staining with a fluorescent FITC conjugate of Annexin V, while propidine iodide can not penetrate the intact cell membrane, but can penetrate cell membrane and stain the karyon for late apoptotic cells or dead cells.

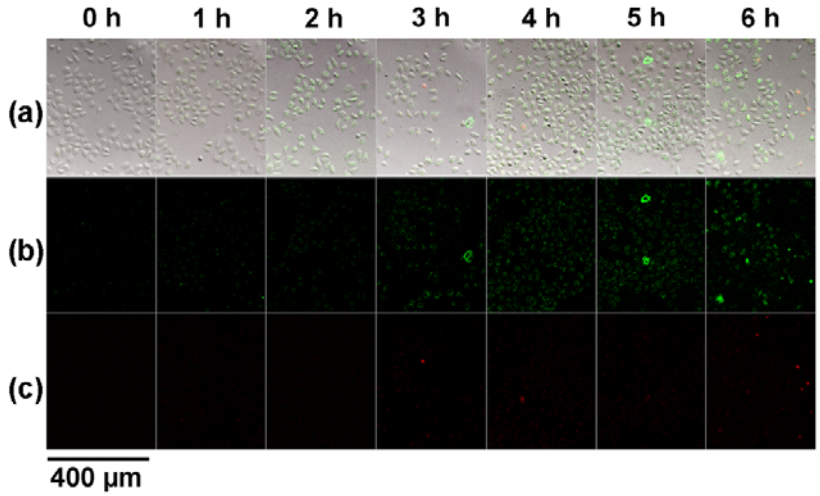

Fig. S7 (a) Brightfield, (b) green channel and (c) red channel confocal fluorescent images of BGC cells exposed to 25 °C PBS from 0 to 6 h, stained with Annexin V-FITC apoptosis detection kit.

Effect of paclitaxel on cell height change

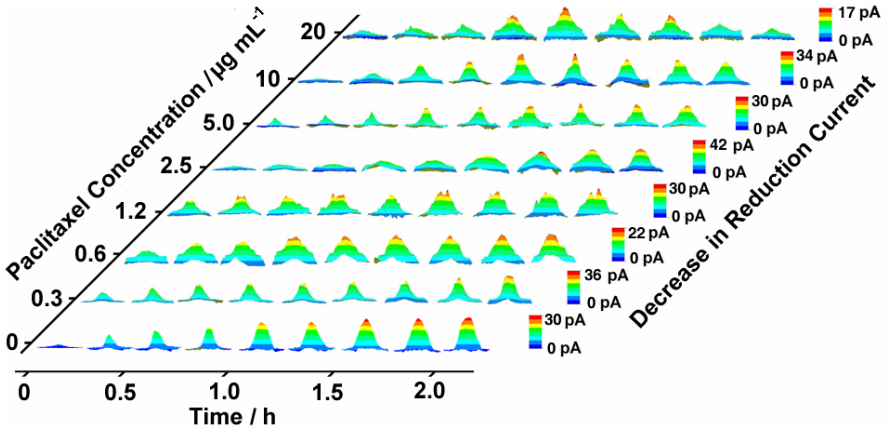

Fig. S8 3D SECM images of BGC cells treated with paclitaxel at concentrations from 0 to 20 μg mL^{-1} in 25 °C PBS. Each line shows the sequential images obtained with a 400-nm-radius Pt tip at every 15 min in 2 h. Conditions: tip potential, −0.4 V *vs.* Ag/AgCl; scan rate, 25 μm s^{-1}; rest time, 2 min. The steady-state currents in bulk solution were 169 ± 2 pA for all the measuements.

Drug sensitivity test by MTT assay

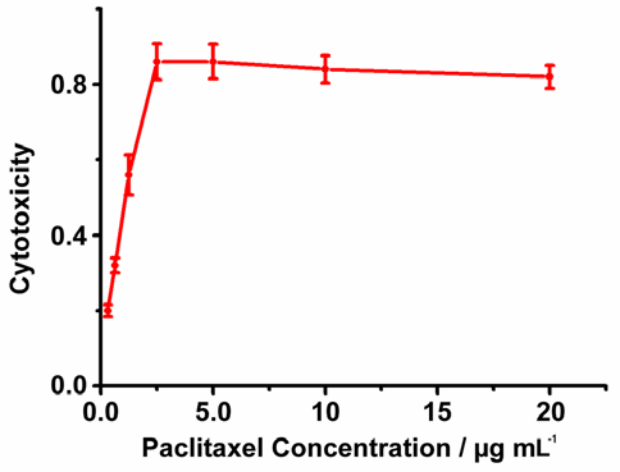

Fig. S9 Cytotoxicity curve obtained by MTT assay for 72 h exposure of BGC cells to paclitaxel.

References

1 J. Chen, D. Du, F. Yan, H. X. Ju and H. Z. Lian, *Chem. Eur. J.*, 2005, **11**, 1467–1472.

2 K. Aoki, K. Akimoto, K. Tokuda, H. Matsuda and J. Osteryoung, *J. Electroanal. Chem.*, 1984, **171**, 219–230.